Inorg. Chem. **2007**, *46*, 3017–3026

Generation and Characterization of $[(P)M–(X)–Co(TMPA)]^{n+}$ Assemblies; P = Porphyrinate, M = Fe^{III} and Co^{III}, X = O^{2-}, OH^-, O_2^{2-}, and TMPA = Tris(2-pyridylmethyl)amine

Eduardo E. Chufán,[†] Claudio N. Verani,[†,‡] Simona C. Puiu,[†] Eva Rentschler,[§,||] Ulrich Schatzschneider,[§,||] Christopher Incarvito,[⊥] Arnold L. Rheingold,[⊥,#] and Kenneth D. Karlin*[,†]

Department of Chemistry, The Johns Hopkins University, Baltimore, Maryland 21218, Max-Planck-Institut für Strahlenchemie, D-45470 Mülheim/Ruhr, Germany, and Chemistry & Biochemistry Department, University of Delaware, Newark, Delaware 19716

Received September 6, 2006

With the established chemistry of bridged $[(porphyrinate)Fe^{III}–X–Cu^{II}(ligand)]^{n+}$ [X = O^{2-} (oxo), OH^- (hydroxo), O_2^{2-} (peroxo)] complexes, we investigated the effect of cobalt ion substitution for copper or copper and iron. Thus, in this report, the generation and characterization of new μ-oxo, μ-hydroxo, and μ-peroxo (μ-X) assemblies of $[(porphyrinate)M^{III}–X–Co^{II/III}(TMPA)]^{n+}$ assemblies is described, where M = Fe^{III} or Co^{III} and TMPA = tris(2-pyridylmethyl)amine. The μ-oxo complex $[(F_8TPP)Fe^{III}–O–Co^{II}(TMPA)]^+$ (**1**, F_8TPP = tetrakis(2,6-difluorphenyl)-porphyrinate) was isolated by an acid–base self-assembly reaction of a 1:1 mixture of $(F_8TPP)Fe^{III}–OH$ and $[Co^{II}(TMPA)(MeCN)]^{2+}$ upon addition of triethylamine. The crystal structure of **1**·$2C_4H_{10}O$ proved the presence of an unsupported Fe–O–Co moiety; ∠Fe–O–Co = 171.6° and *d*(Fe···Co) = 3.58 Å. Complex **1** was further characterized by UV–vis (λ_{max} = 437 (Soret) and 557 nm), ^{1}H NMR [δ 40.6 (pyrrole-H), 8.8 and 8.7 (*m*-phenyl-H), 8.0 (*p*-phenyl-H), 4.4 (PY-4H), 2.6 (PY-3H), 1.0 (PY-5H), –1.1 (PY-6H), and –2.7 (TMPA–CH_2–) ppm], electrospray ionization (ESI) and matrix-assisted laser desorption ionization time-of-flight (MALDI-TOF) mass spectrometric methods, Evans method NMR (μ_{eff} = 3.1), and superconducting quantum interference device (SQUID) susceptometry (J = –114 cm^{-1}, S = 1). The μ-hydroxo analogue $[(F_8TPP)Fe^{III}–(OH)–Co^{II}(TMPA)]^+$ (**2**) [UV–vis λ_{max} = 567 nm; δ 78 ppm (pyrrole-H); Evans NMR μ_{eff} = 3.7] was generated by addition of 1 equiv of triflic acid to **1**. The protonation is completely reversible, and **1** is regenerated from **2** by addition of triethylamine. While $(F_8TPP)Fe^{II}/[Co^{II}(TMPA)-(MeCN)]^{2+}/O_2$ chemistry does not lead to a stable μ-peroxo species, a dicobalt μ-peroxo complex $[(TPP)Co^{III}–(O_2^{2-})–Co^{III}(TMPA)]^{2+}$ (**3**, TPP = *meso*-tetraphenylporphyrinate) forms from a reaction of O_2 with a 1:1 mixture of the Co^{II} precursor components at –80 °C [UV–vis λ_{max} = 435 (Soret), 548, and 583 (weak) nm; silent EPR spectrum; diamagnetic NMR spectrum]. The oxygenation/deoxygenation equilibrium is reversible; warming solutions of **3** releases ~1 equiv of O_2 and the reduced complexes are reformed.

Introduction

In the past few years we have studied a series of μ-peroxo and μ-oxo heme−copper complexes, aimed at providing basic insights into dioxygen activation by enzymes such as cytochrome *c* oxidase.[1,2] These complexes are formed by reacting dissimilar copper−polypyridine and iron−porphyrinate building blocks; the products include $[(F_8TPP)Fe^{III}–(O_2^{2-})–Cu^{II}(TMPA)]^+$ and $[(F_8TPP)Fe^{III}–O–Cu^{II}(TMPA)]^+$ (Chart 1, F_8TPP = tetrakis(2,6-difluorphenyl)porphyrinate, and TMPA = tris(2-pyridylmethyl)amine). The μ-peroxo complex results from the reaction of molecular dioxygen with the reduced components $[Fe^{II}(F_8TPP)]$ and $[Cu^{I}(TMPA)-$

* To whom correspondence should be addressed. E-mail: karlin@jhu.edu.
† The Johns Hopkins University.
‡ Present address: Department of Chemistry, Wayne State University, Detroit, MI 48207.
§ Max-Planck-Institut.
|| Present address: Institute for Inorganic Chemistry, Gutenberg University, D-55099 Mainz, Germany.
⊥ University of Delaware.
Present address: Chemistry Department, University of California, San Diego, La Jolla, CA 92093.

(1) Kim, E.; Chufán, E. E.; Kamaraj, K.; Karlin, K. D. *Chem. Rev.* **2004**, *104*, 1077−1133.
(2) Karlin, K. D.; Kim, E. *Chem. Lett.* **2004**, *33*, 1226−1231.

10.1021/ic061686k CCC: $37.00
Published on Web 03/20/2007

Chart 1

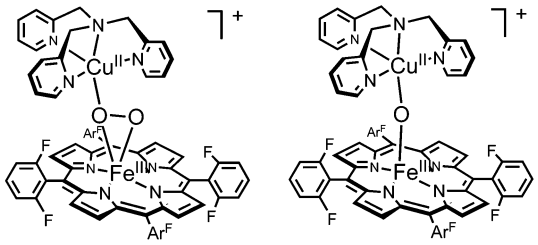

$[(F_8TPP)Fe\text{-}(O_2^{2-})\text{-}Cu(TMPA)]^+$ $[(F_8TPP)Fe\text{-}(O^{2-})\text{-}Cu(TMPA)]^+$

(MeCN)]$^+$ (Me = methyl) at low temperatures, and it is subsequently converted to a μ-oxo species upon temperature increase.[3] Independent syntheses of μ-oxo complexes could be successfully achieved through an "acid−base" self-assembly approach in which another building block, namely, $[(F_8TPP)Fe^{III}-OH]$ was treated with $[Cu^{II}(TMPA)(MeCN)]^{2+}$ in the presence of base to yield $[(F_8TPP)Fe^{III}-O-Cu^{II}(TMPA)]^+$.[4] Analogue μ-oxo complexes having tridentate chelates (bis-(2-pyridylethyl)-methylamine)[5] or that with dimethylamino 4-pyridyl substituents[6] as the Cu(II) ligand have similarly been synthesized and characterized. Recent extended X-ray absorption fine structure (EXAFS) spectroscopy and density functional theory (DFT) calculations[7] indicate that $[(F_8TPP)Fe^{III}-(O_2^{2-})-Cu^{II}(TMPA)]^+$ possesses a $\mu-\eta^2:\eta^1$-peroxo bridging geometry similar to that observed for a X-ray structurally characterized complex studied by Naruta and co-workers.[8] $[(F_8TPP)Fe^{III}-O-Cu^{II}(TMPA)]^+$ (Chart 1) has been thoroughly characterized (including by X-ray diffraction) and possesses a near-linear Fe−O−Cu moiety.[9]

In this account, we present the results obtained through related broad approaches employing acid−base self-assembly or metal−dioxygen reactivity strategies, but now involving substitution of cobalt, either for the heme or for the copper ion center. A new μ-oxo species $[(F_8TPP)Fe^{III}-O-Co^{II}(TMPA)](ClO_4)$ (**1**) has been isolated from acid−base synthesis and its X-ray structure, spectroscopic, and magnetic properties are described in detail. The protonation chemistry of this compound was also investigated, yielding the μ-hydroxo analogue $[(F_8TPP)Fe^{III}-(OH)-Co^{II}(TMPA)]^{2+}$ (**2**). In fact, a dioxygen adduct formulated as the μ-peroxo dicobalt(III) species $[(TPP)Co^{III}-(O_2^{2-})-Co^{III}(TMPA)]^{2+}$ (**3**) is also described.

Scheme 1

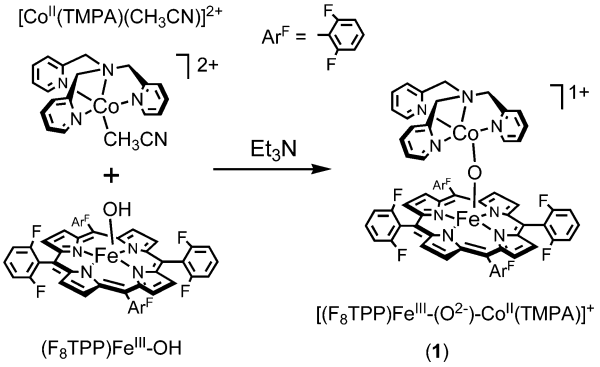

$(F_8TPP)Fe^{III}\text{-}OH$ (**1**)

Cobalt substituted hemes, both natural and synthetic, have been studied extensively to elucidate fundamental metalloporphyrin chemistry, including O_2-binding.[10−14] As concerns analogues of heme−Cu cytochrome *c* oxidase models, Collman[15,16] and Boitrel[17] also used Co-for-Fe and Co-for-Cu substitutions. With a tetraphenylporphyrinate covalently linked to a triazacyclononane or with imidazole-picket porphyrins, Collman and co-workers synthesized binuclear (porphyrinate)Co^{II}/Cu^{I} compounds that react with O_2 to yield different products; a peroxo-bridged $[Co^{III}-(O_2^{2-})-Cu^{II}]$[15] and a cobalt-superoxo $[Co^{III}-(O_2^{-})\cdots Cu^{I}]$[16] species were formed, respectively. Boitrel and co-workers described a Co^{II}/Co^{II} cyclam-strapped porphyrin that in the presence of excess bulky base reacts with O_2 to form a peroxo-bridged $[Co^{III}-(O_2^{2-})-Co^{III}]$ complex.[17]

Results and Discussion

Synthesis of 1. The acid−base synthesis used to generate **1** is described in Scheme 1. Triethylamine was added to a 1:1 mixture of $(F_8TPP)Fe^{III}-OH$ and $[Co^{II}(TMPA)(MeCN)]^{2+}$ (as perchlorate salt, see Experimental Section) to deprotonate the hydroxyl group attached to the iron center thereby enabling adduct formation.[4] This reaction was followed by UV−vis spectroscopy. The initial and final spectra are shown in Figure 1. Note that the initial spectrum is dominated by the intense bands associated with $(F_8TPP)Fe^{III}-OH$. Electrospray ionization (ESI) and matrix-assisted laser desorption ionization time-of-flight (MALDI-TOF)

(3) Ghiladi, R. A.; Hatwell, K. R.; Karlin, K. D.; Huang, H.-w.; Moënne-Loccoz, P.; Krebs, C.; Huynh, B. H.; Marzilli, L. A.; Cotter, R. J.; Kaderli, S.; Zuberbühler, A. D. *J. Am. Chem. Soc.* **2001**, *123*, 6183−6184.

(4) Fox, S.; Nanthakumar, A.; Wikström, M.; Karlin, K. D.; Blackburn, N. J. *J. Am. Chem. Soc.* **1996**, *118*, 24−34.

(5) Kopf, M.-A.; Neuhold, Y.-M.; Zuberbühler, A. D.; Karlin, K. D. *Inorg. Chem.* **1999**, *38*, 3093−3102.

(6) Kim, E.; Helton, M. E.; Wasser, I. M.; Karlin, K. D.; Lu, S.; Huang, H.-w.; Moënne-Loccoz, P.; Incarvito, C. D.; Rheingold, A. L.; Honecker, M.; Kaderli, S.; Zuberbühler, A. D. *Proc. Natl. Acad. Sci. U.S.A.* **2003**, *100*, 3623−3628.

(7) del Rio, D.; Sarangi, R.; Chufán, E. E.; Karlin, K. D.; Hedman, B.; Hodgson, K. O.; Solomon, E. I. *J. Am. Chem. Soc.* **2005**, *127*, 11 969−11 978.

(8) Chishiro, T.; Shimazaki, Y.; Tani, F.; Tachi, Y.; Naruta, Y.; Karasawa, S.; Hayami, S.; Maeda, Y. *Angew. Chem. Int. Ed.* **2003**, *42*, 2788−2791.

(9) Karlin, K. D.; Nanthakumar, A.; Fox, S.; Murthy, N. N.; Ravi, N.; Huynh, B. H.; Orosz, R. D.; Day, E. P. *J. Am. Chem. Soc.* **1994**, *116*, 4753−4763.

(10) Hoffman, B. M.; Petering, D. H. *Proc. Natl. Acad. Sci., U.S.A.* **1970**, *67*, 637−ff.

(11) Doyle, M. L.; Speros, P. C.; Licata, V. J.; Gingrich, D.; Hoffman, B. M.; Ackers, G. K. *Biochemistry* **1991**, *30*, 7263−7271.

(12) Venkatesh, B.; Manoharan, P. T.; Rifkind, J. M. Metal ion reconstituted hybrid hemoglobins, In *Progress in Inorganic Chemistry*, Vol 47; Karlin, K. D., Ed.; John Wiley & Sons Inc: New York, 1998; pp 563−684.

(13) Proniewicz, L. M.; Kincaid, J. R. *Coord. Chem. Rev.* **1997**, *161*, 81−127.

(14) Bruha, A.; Kincaid, J. R. *J. Am. Chem. Soc.* **1988**, *110*, 6006−6014.

(15) Collman, J. P.; Fu, L.; Herrmann, P. C.; Zhang, X. *Science* **1997**, *275*, 949−951.

(16) Collman, J. P.; Berg, K. E.; Sunderland, C. J.; Aukauloo, A.; Vance, M. A.; Solomon, E. I. *Inorg. Chem.* **2002**, *41*, 6583−6596.

(17) Andrioletti, B.; Ricard, D.; Boitrel, B. *New J. Chem.* **1999**, *23*, 1143−1150.

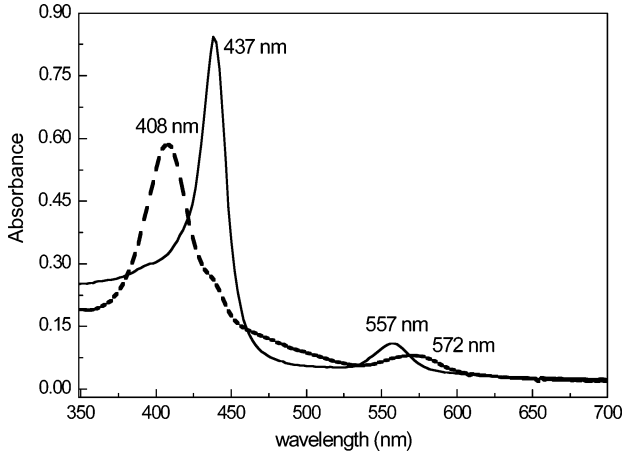

Figure 1. UV−vis spectra of the mixture of $(F_8TPP)Fe^{III}$−OH/$[Co^{II}$-(TMPA)(MeCN)$]^{2+}$ (- - -) and the μ-oxo product **1** (—) upon addition of 1 equiv of Et_3N in CH_2Cl_2 at room temperature.

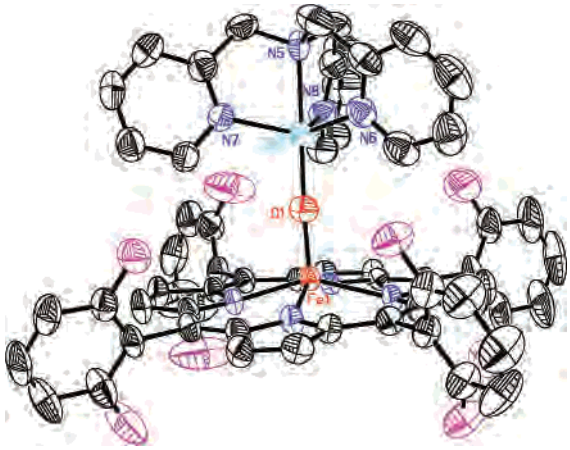

Figure 2. An ORTEP representation of the cationic portion of (**1**)·ClO_4·$2C_4H_{10}O$. Fe···Co = 3.58 Å, Co(1)−O(1) = 1.85 Å, Co(1)−N(8) = 2.06 Å, Co(1)−N(7) = 2.07 Å, Co(1)−N(6) = 2.09 Å, Co(1)−N(5) = 2.18 Å, Fe(1)−O(1) = 1.75 Å, Fe(1)−N(4) = 2.10 Å, Fe(1)−N(3) = 2.10 Å, Fe(1)−N(1) = 2.11 Å, Fe(1)−N(2) = 2.12 Å, ∠Fe−O−Co = 171.6°. The crystallographic data and structural refinement parameters are reported in Table S1 (Supporting Information).

mass spectrometry (Experimental Section) were used to evaluate the integrity of the species both in a solution and as a solid. In solution, a cluster of peaks at m/z = 1176−1179 are ascribed to the cationic species $[(F_8TPP)Fe^{III}$−O−$Co^{II}(TMPA)]^+$, which can only be simulated by taking into account the isotopic distribution for both cobalt and iron centers (see Supporting Information, Figures S1 and S2).

X-ray Structure of 1. $[(F_8TPP)Fe^{III}$−O−$Co^{II}(TMPA)]$-ClO_4·$2C_4H_{10}O$ was crystallized from dichloromethane/diethyl ether at −20 °C. An Oak Ridge thermal ellipsoid plot (ORTEP) diagram is shown in Figure 2 with key bond distances provided; Fe···Co = 3.58 Å. The cation exhibits a slightly bent [Fe−O−Co] core, with ∠Fe−O−Co = 171.6°. For similar systems containing the $[Fe^{III}$−O−$Cu^{II}]$ core in which the copper ion is capped by tetradentate N_4-ligands, compounds from our own research and that of Holm and co-workers, this value is found to lie in the range 175−178°.[1] The ∠Fe−O−Co angle in **1** most closely compares to that found for $[(^6L)Fe$−O−$Cu]^+$ (∠Fe−O−Cu = 171°), which possesses a TMPA moiety bound to copper(II) but where the chelate is tethered covalently to the porphyrinate periphery (i.e., in the so-called ^6L ligand). An exceptional case is for a complex $[(^5L)Fe$−O−$Cu]^+$ (∠Fe−O−Cu = 141°, based on EXAFS multiple scattering analysis;[18] ^5L is also a heterobinucleating ligand, see ref 1), where severe ^5L binucleating ligand constraints force strong distortions. Thus, only minor distortions from linear occur in **1**.

The high-spin Fe^{III} (vide infra) is bound to the porphyrin macrocycle and exhibits a typical square pyramidal geometry, being displaced by 0.56 Å above the ligand plane. The bridging oxo atom occupies the apical position, with an Fe−O distance of 1.75 Å being close to analogues containing [Fe−O−Cu] and [Fe−O−Fe] cores.[1,19] All Fe−N distances are within the range of 2.10−2.12 Å, which is consistent with a high-spin electronic configuration for a $3d^5$ Fe^{III} ion.[20] The cobalt center is surrounded by three methyl-pyridyl groups attached to an amine that occupies the axial position for the ion. The $Co-N_{Py}$ distances are within 2.06−2.09 Å, whereas the apical amino-nitrogen is found at 2.18 Å, and the Co−O distance is 1.85 Å. The N_{amino} and the O_{oxo} ligands occupy the apical positions of a trigonal bipyramid, conferring a local C_{3v} symmetry for this metal. It is evident that the overall geometry around the cobalt ion in **1** is preserved compared to its precursor complex $[Co^{II}(TMPA)(MeCN)]^{2+}$.[21] The apical Co−N bond length is unchanged while the Co−$N_{pyridyl}$ bond distances increase slightly in **1**.

As expected, the $Co-O_{oxo}$ distance (1.85 Å) in **1** is shorter than the $Co-N_{acetonitrile}$ bond length in $[Co^{II}(TMPA)$-$(MeCN)]^{2+}$ (2.05 Å), due to the electrostatic nature of the interaction. This $Co-O_{oxo}$ moiety is also found in other kinds of oxo-bridged compounds that exhibit a square-planar Co_2^{III}-(μ-oxo)$_2$ core ($Co-O_{average}$ = 1.80 Å, varying from 1.78 to 1.83 Å).[22−24] The slightly longer bond in the presently described Co^{II}−oxo−Fe^{III} core of **1** can, of course, be attributed to the presence of a lower oxidation state metal ion (i.e., Co^{II} and not Co^{III}). Interestingly, the $Cu^{II}-O_{oxo}$ bond lengths of a variety of heme−O−Cu^{II} assemblies fall in the narrow range of 1.83−1.86 Å,[1] which is the same as that of the present cobalt case; thus, the smaller ionic radius of Cu^{II} relative to Co^{II} is not reflected.

NMR Spectroscopic and Magnetic Properties. ^1H NMR spectra of $(F_8TPP)Fe^{III}$−OH in CD_2Cl_2 exhibit a pyrrole signal at 81 ppm, typical for high-spin S = 5/2 Fe^{III}-porphyrinates.[9] Following the reaction with $[Co^{II}(TMPA)(CH_3$-$CN)]^{2+}$ and formation of **1**, the pyrrole resonance appears upfield at 40.6 ppm (Figure 3). This behavior is consistent with an assignment of **1** as an S = 1 electronic ground state species, which is derived from antiferromagnetic coupling

(18) Obias, H. V.; van Strijdonck, G. P. F.; Lee, D.-H.; Ralle, M.; Blackburn, N. J.; Karlin, K. D. *J. Am. Chem. Soc.* **1998**, *120*, 9696−9697.
(19) Kurtz, D. M., Jr. *Chem. Rev.* **1990**, *90*, 585−606.
(20) Scheidt, W. R.; Reed, C. A. *Chem. Rev.* **1981**, *81*, 543−555.
(21) Nanthakumar, A.; Fox, S.; Murthy, N. N.; Karlin, K. D. *J. Am. Chem. Soc.* **1997**, *119*, 3898−3906.
(22) Dai, X. L.; Kapoor, P.; Warren, T. H. *J. Am. Chem. Soc.* **2004**, *126*, 4798−4799.
(23) Larsen, P. L.; Parolin, T. J.; Powell, D. R.; Hendrich, M. P.; Borovik, A. S. *Angew. Chem. Int. Ed.* **2003**, *42*, 85−89.
(24) Hikichi, S.; Yoshizawa, M.; Sasakura, Y.; Akita, M.; Moro-Oka, Y. *J. Am. Chem. Soc.* **1998**, *120*, 10 567−10 568.

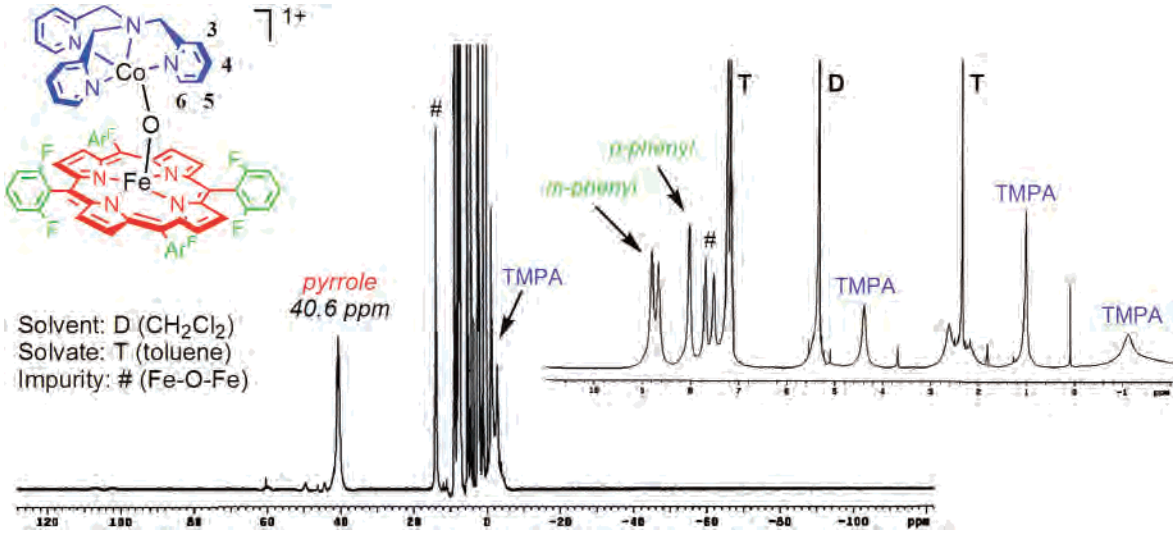

Figure 3. ^{1}H NMR spectrum (CD_2Cl_2, 293 K) of **1**. See text for further discussion and assignments.

of the high-spin Fe^{III} ($S = 5/2$) and high-spin Co^{II} ($S = 3/2$) through the oxo bridging ligand. Magnetization studies corroborate this conclusion (vide infra). The same upfield shifting of $\delta_{pyrrole}$ (from 81 ppm) was observed for the copper analogue $[(F_8TPP)Fe^{III}-O-Cu^{II}(TMPA)]^+$, but the magnitude of the shift was much lower because of the different electronic nature of Cu^{II} ($S = 1/2$) that yields a different ground state ($S = 2$, $\delta_{pyrrole} = 65$ ppm). On the other hand, the porphyrin signals due to the *meso*-phenyl substituents appear at $\delta = 8.8$ and 8.7 ppm for the meta-positions and at $\delta = 8.0$ ppm for the para-position, as is usual for metal tetraaryl-porphyrinates.[21]

$[Co^{II}(TMPA)(CH_3CN)]^{2+}$ itself exhibits considerably shifted but sharp ($\tau_s \approx 10^{-11}$ s for Co^{II}) contact-shifted ^{1}H NMR signals.[21] From the present study, we discovered that there were modest errors in the resonances that we previously[21] reported for this complex, and with new, careful, and multiple measurements, we find that TMPA hydrogen signals occurred at 109.1 ($-CH_2-$), 60.7 (5-H), 41.6 (3-H), and -4.6 (4-H) ppm in dichloromethane, see the spectrum in Figure S3 (Supporting Information). For **1**, all of these signals moved as expected for a magnetically coupled system, with the peaks occurring at 4.4 (4-H), 2.6 (3-H), 1.0 (5-H), -1.1 (6-H, shifted dramatically from >125 ppm downfield in $[Co^{II}(TMPA)(CH_3CN)]^{2+}$), and -2.7 ($-CH_2-$) ppm. These tentative assignments (in parentheses) are based on analogy to the $Fe^{III}-O-Cu^{II}$ system[21] and on the observed temperature dependent behavior (see below). Thus, variable temperature NMR studies were carried out for **1** (see Figure S4, Supporting Information), and revealed that the pyrrole downfield-shifted signal moved further downfield with the decrease in temperature while the TMPA hydrogen upfield-shifted signals moved further upfield. This phenomenon was also observed for the coupled copper containing μ-oxo compound $[(F_8TPP)Fe^{III}-O-Cu^{II}(TMPA)]^+$, thus being consistent with strong antiferromagnetic coupling.[21] Plots of chemical shift vs $1/T$ for the range 193−293 K (see Figure S5, Supporting Information) show linear Curie and anti-Curie behavior for the iron−porphyrinate and Co(TMPA) protons, respectively. The room-temperature TMPA peaks at -1.1 and -2.7 ppm assigned to the 6-H and $-CH_2-$ hydrogens, respectively, are the most affected by the lowering of the temperature (-10.2 and -12.6 ppm at -80 °C, respectively) because they are the hydrogen atoms closest to the paramagnetic Co^{II} center. Also, they have positive extrapolated intercepts (see Curie plot), which are consistent with the breaking of the strong antiferromagnetic coupling as the temperature increases and (theoretically) approaches infinity.

Other relevant information obtained from the NMR data relates to the coupled structure of $Fe^{III}-O-Co^{II}$ that remains undissociated in CH_2Cl_2 solution. Nonetheless, dissociation does occur in CH_3CN, as indicated by the formation of $(F_8TPP)Fe^{III}-OH$, observed with $\delta_{pyrrole} = 81$ ppm (not shown).

Magnetic Susceptibility. Data for polycrystalline **1** were collected in the temperature range of 2−290 K (Figure 4) and were aimed at the evaluation of the magnetic exchange interaction described by the coupling constant (J) resulting from the possibility of either or both antiferromagnetic (AF) and ferromagnetic (F) exchange interactions, with $J = J_{AF} + J_F$.

At 290 K, the compound exhibits $\chi_{mol}T = 2.06$ emu K·mol^{-1}, therefore much lower than the expected value of 6.25 emu K·mol^{-1} for a bimetallic system with $S_{Fe} = 5/2$ and $S_{Co} = 3/2$. By decreasing the temperature to 20 K, the values of $\chi_{mol}T$ decrease monotonically, with $\chi_{mol}T$ values varying from 2.02 to 1.46 emu K·mol^{-1}. Further cooling causes an abrupt inflection that reaches $\chi_{mol}T = 0.93$ emu K·mol^{-1}, which is in agreement with an $S = 1$ ground state. The best fit yields $J = -114$ cm^{-1}, with $g_{Fe} = g_{Co} = 2.5$, and confirms the AF nature of the coupling. The elevated values of the g-factor may reflect spin−orbit contributions expected for a system containing d^7 ions. The fact that neither the Co^{II} nor the Fe^{III} ions stand in an octahedral geometry can also contribute to elevated g-values. Complex **1** approaches an overall low-symmetry C_s, with local C_{3v} trigonal bipyramidal symmetry for the Co^{II} ion and square pyramidal C_{4v} local Fe^{III} geometry. The high-spin configurations for both ions deviate considerably from the usual octahedral

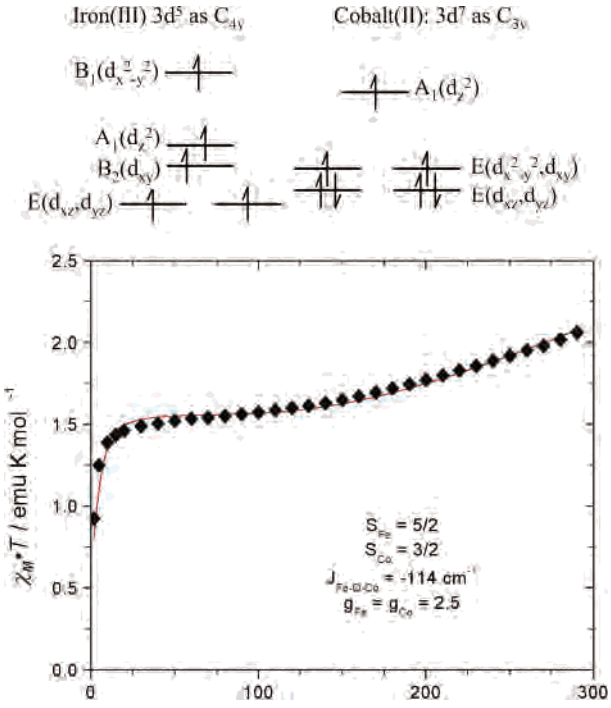

Figure 4. Magnetochemical behavior of complex **1** ($\chi_{mol}T$ vs temperature, *T*). The black diamonds denote the measured magnetization and the solid red line is the simulation of the data. The high-spin electronic configurations for the metal ions are also shown at the top.

scheme and need to be taken into account for an evaluation of the magnetic pathway. On the basis of orbital distribution arguments and the X-ray structure, it is well-established that the A_1 (d_z^2) orbital of the iron center will be pointing out of the macrocyclic plane. Similarly, DFT calculations for the precursor $[Co^{II}(TMPA)(CH_3CN)]^+$ indicate that the *z*-axis, as would be expected, is clearly defined along the $N_{amine}-Co-N_{acetonitrile}$ in this trigonal bypyriamidal complex.[25] As such, the main superexchange pathway for the dominant AF coupling observed for **1** is σ in nature.

In fact, the exchange coupling constant for **1** ($J = -114$ cm^{-1}) is comparable to that found for the iron analogue $[(F_8TPP)Fe^{III}-O-Fe^{III}(TMPA)(Cl)]^+$ ($J = -108$ cm^{-1}).[26] Here, a high-spin Fe^{III} ion replaces the Co^{II} ion in a very similar coordination environment. However, for the previously well-studied analogue $[(F_8TPP)Fe^{III}-O-Cu^{II}(TMPA)]^+$, where Cu^{II} ions replace the Co^{II} ion, a stronger coupling is observed, $J = -174$ cm^{-1}.[9] This result may be general in that the $Fe^{III}-O-Cu^{II}$ core also possesses larger $|J|$ values, as $J \geq |-200|$ cm^{-1} for both $[(OEP)Fe^{III}-O-Cu^{II}(Me_6tren)]^+$ and for $[(^6L)-Fe^{III}-O-Cu^{II}]^+$.[1]

Protonation of 1. The Brønsted basic behavior of oxo-bridged heme-containing bimetallic complexes has been observed for compounds with iron−copper, iron−iron, and other $[M_A-O-M_B]$ cores.[1,27] Furthermore, a reversible oxo/hydroxo equilibrium has been demonstrated for $[(F_8TPP)-Fe^{III}-O(H)-Cu^{II}(ligand)]^{n+}$ (ligand = TMPA[4] or bis(2-(2-pyridyl)ethyl)amine[5]) complexes; the hydroxo-bridged complexes formed by protonation of the μ-oxo compounds can be reconverted to the original oxo species by means of addition of a base such as triethylamine.[4] Therefore, the reaction of **1** with triflic acid/triethylamine was investigated in order to assess and compare its protonation/deprotonation profile with that of other compounds, especially $[(F_8TPP)-Fe^{III}-O-Cu^{II}(TMPA)]^+$.

Scheme 2

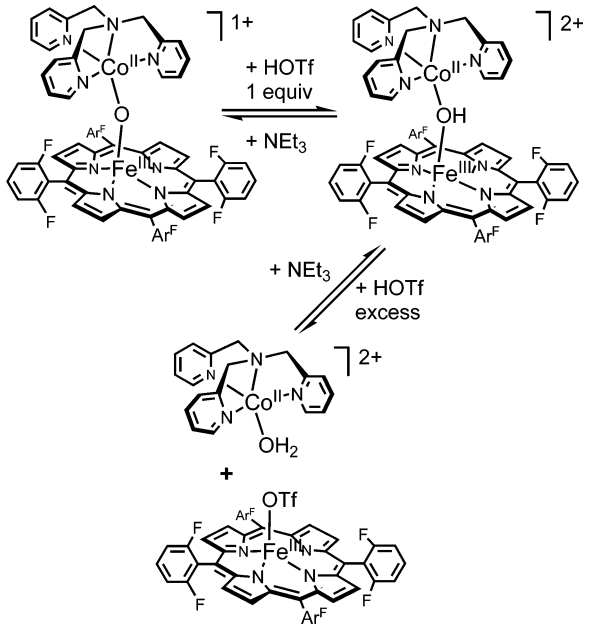

Addition of 1 equiv of triflic acid to a dichloromethane solution of **1** ($\lambda_{max} = 557$ nm) yields a new UV−vis spectrum ($\lambda_{max} = 567$ nm) attributed to a μ-hydroxo species $[(F_8TPP)-Fe^{III}-(OH)-Co^{II}(TMPA)]^{2+}$ (**2**), shown in Scheme 2. After addition of 1 equiv of triethylamine, the original spectrum of **1** is observed. This cycle of protonation/deprotonation can be repeated three times without detecting significant decomposition (see Supporting Information, Figure S6).

^{1}H NMR spectroscopy was used to further investigate this reaction and characterize the protonated product (Figure 5). After addition of 0.45 equiv of triflic acid (HOTf) to a dichloromethane-d_2 solution of **1**, a new pyrrole-associated broad signal is observed at 78 ppm while the original signal at 40.5 ppm (due to **1**) is diminished. The reaction is almost complete with the addition of 0.9 equiv of the acid (Figure 5). This new signal at 78 ppm relates quite well to the typical pyrrole signal of $(F_8TPP)Fe^{III}-OH$ normally found at 81 ppm,[9] but here it is measurably shifted upfield, reflecting the AF coupling to the cobalt center in **2**.

To further provide evidence that the protonation product is a hydroxo-bridged compound, the magnetic moment of the starting compound and the products were determined by the Evans NMR method (see Experimental Section). Complex **1** exhibits $\mu_{eff} = 3.1$ that is consistent with that expected for a $S = 1$ system (vide supra). After addition of 1 equiv of triflic acid, a value of $\mu_{eff} = 3.7$ is observed. This magnetic moment is also consistent with an $S = 1$ system arising from an AF coupling between a high-spin Fe^{III} and a high-spin

(25) Schatzschneider, U.; Verani, C. N.; Karlin, K. D., et al, unpublished observations.
(26) Wasser, I. M.; Martens, C. F.; Verani, C. N.; Rentschler, E.; Huang, H. W.; Moenne-Loccoz, P.; Zakharov, L. N.; Rheingold, A. L.; Karlin, K. D. *Inorg. Chem.* **2004**, *43*, 651−662.
(27) Kramarz, K. W.; Norton, J. R. In *Progress in Inorganic Chemistry*, Vol 42; John Wiley & Sons Inc: New York, 1994;pp 1−65.

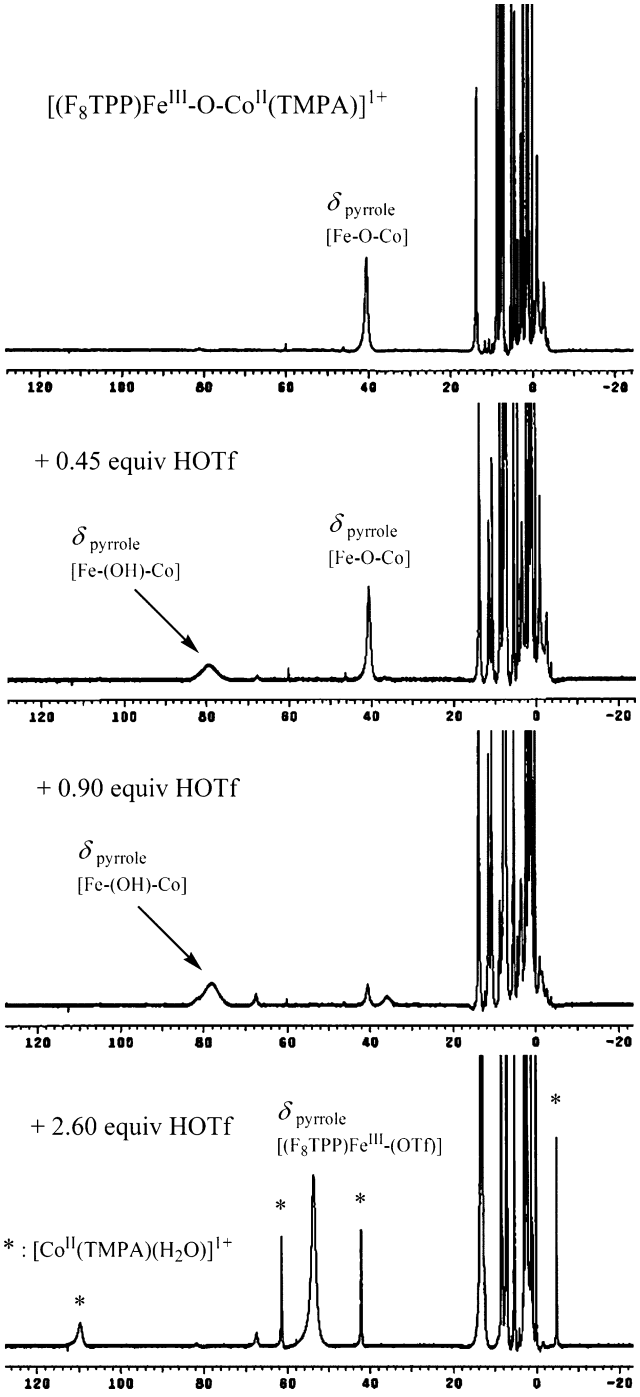

Figure 5. Protonation of **1** by sequentially adding 0.45 equiv, 0.90 equiv, and excess (2.60 equiv) triflic acid followed by ^{1}H NMR spectroscopy (CD_2Cl_2, room temperature). ^{1}H NMR spectra showing the expanded −2 to 15 ppm region are provided in Supporting Information, Figure S7.

Co^{II}; however, the coupling is less effectively propagated when mediated by a μ-hydroxo group compared to a μ-oxo ligand.[1] This follows what was previously observed for μ-oxo and μ-hydroxo [(heme)Fe^{III}−O(H)−Cu^{II}(ligand)] pairs of complexes.[1,28] While we do not currently have X-ray or other structural information pertaining to the μ-OH^- complex **2**, we can expect longer iron−hydroxo and cobalt−hydroxo bond distances compared to an oxo analogue, and bending of the Fe−(OH)−Co core is also likely (as one goes from formally sp hydridized oxo to sp^2 hybridized hydroxo ligands).[4,29]

After addition of excess triflic acid (2.6 equiv), (F_8TPP)-Fe^{III}−(OTf) ($\delta_{pyrrole}$ = 53 ppm) is identified,[30] further showing that the 78 ppm resonance ascribed to **2** is correct and that the bridge has not been broken in this product. [Co^{II}(TMPA)-(H_2O)]$^{2+}$ is the presumed coproduct (see Figure 5 for ^{1}H NMR spectroscopic identification) (Scheme 2), having the same pyridyl-ligand chemical shift as that previously found for the close acetonitrile analogue [Co^{II}(TMPA)(CH_3CN)]$^{2+}$ (vide supra, Figure 3). The magnetic moment of the product solution, μ_{eff} = 6.7, is consistent with that of an uncoupled mixture of an admixed-spin-state Fe^{III} compound (S = 5/2,3/2) expected for (F_8TPP)Fe^{III}−(OTf)[30] and a high-spin Co^{II} complex (theoretical μ_{eff} = 6.81).

To further investigate the nature of this second equilibrium where bridging ligand cleavage occurs (Scheme 2), an UV−vis spectroscopic experiment was carried out. Following the addition of 2 equiv of HOTf to a solution of **1** (CH_2Cl_2, λ_{max} = 558 nm), the characteristic[30] spectrum of (porphyrinate)−Fe^{III}−(weak-anion) (e.g., weak-anion = OTf^-, ClO_4^-, BF_4^-) complex [(F_8TPP)Fe^{III}−triflate] is formed (λ_{max} = 504, 572, and 635 nm) (see Supporting Information, Figure S8). Reversible generation of the original oxo-bridged compound **1** is observed upon addition of 2 equiv of triethylamine (Figure S8), confirming the weak nature of the Fe^{III}−triflate bond, the full acid−base reversibility in the system (Scheme 2), and therefore the (kinetic or thermodynamic) stability of the μ-oxo/hydroxo assemblies **1** and **2**.

Dioxygen Chemistry of [(F_8TPP)Fe^{II}]/[Co^{II}(TMPA)-(CH_3CN)]$^{2+}$. On the basis of the established O_2 chemistry of (F_8TPP)Fe^{II}/[Cu^{I}(TMPA)(CH_3CN)]$^+$ 1:1 mixtures (also see Introduction),[3] it was envisioned that the substitution of Cu^I by Co^{II} could lead to the generation of a more stable peroxo species by encompassing Fe/Co systems with a $3d^6$ electronic configuration for the cobalt−ligand moiety.[15−17,31−43] Upon

(28) A reviewer has pointed out that the observed value of μ_{eff} = 3.7 may in fact be more consistent with a S = 3/2 assignment. Additional temperature-dependent magnetic susceptibility measurements with greater accuracy would be required to sort this out.

(29) Scott, M. J.; Zhang, H. H.; Lee, S. C.; Hedman, B.; Hodgson, K. O.; Holm, R. H. *J. Am. Chem. Soc.* **1995**, *117*, 568−569.
(30) Boersma, a. D.; Goff, H. M. *Inorg. Chem.* **1982**, *21*, 581−586.
(31) Hu, X. L.; Castro-Rodriguez, I.; Meyer, K. *J. Am. Chem. Soc.* **2004**, *126*, 13 464−13 473.
(32) Gavrilova, A. L.; Qin, C. J.; Sommer, R. D.; Rheingold, A. L.; Bosnich, B. *J. Am. Chem. Soc.* **2002**, *124*, 1714−1722.
(33) Bakac, A. *Prog. Inorg. Chem.* **1995**, *43*, 267−351.
(34) Busch, D. H.; Alcock, N. W. *Chem. Rev.* **1994**, *94*, 585−624.
(35) Solomon, E. I.; Tuczek, F.; Root, D. E.; Brown, C. A. *Chem. Rev.* **1994**, *94*, 827−856.
(36) Suzuki, M.; Furutachi, H.; Okawa, H. *Coord. Chem. Rev.* **2000**, *200−202.*, 105−129.
(37) Hikichi, S.; Akita, M.; Moro-Oka, Y. *Coord. Chem. Rev.* **2000**, *198*, 61−87.
(38) Niederhoffer, E. C.; Timmons, J. H.; Martell, A. E. *Chem. Rev.* **1984**, *84*, 137.
(39) Fallab, S.; Mitchell, P. R. *Adv. Inorg. Bioinorg. Mech.* **1984**, *3*, 311−377.
(40) Collman, J. P.; Yan, Y. L.; Eberspacher, T.; Xie, X.; Solomon, E. I. *Inorg. Chem.* **2005**, *44*, 9628−9630.
(41) Spingler, B.; Scanavy-Grigorieff, M.; Werner, A.; Berke, H.; Lippard, S. J. *Inorg. Chem.* **2001**, *40*, 1065−1066.
(42) Egan, J. W.; Haggerty, B. S.; Rheingold, A. L.; Sendlinger, S. C.; Theopold, K. H. *J. Am. Chem. Soc.* **1990**, *112*, 2445−2446.

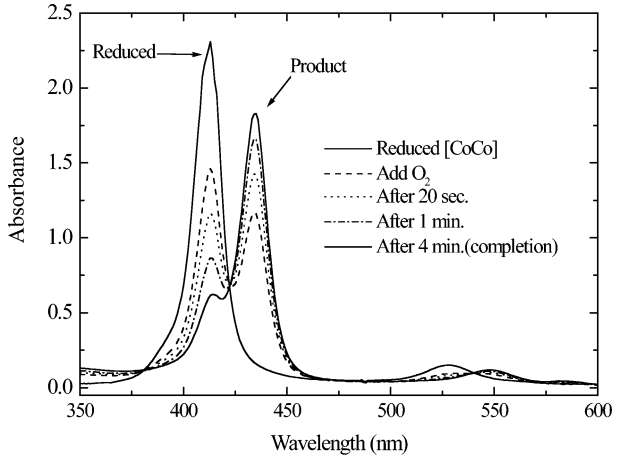

Figure 6. An UV−vis spectra of the mixture of [(TPP)Co^{II}]/[Co^{II}(TMPA)-(MeCN)]$^{2+}$ (reduced species) and of the product **3** upon reaction with O_2 at −80 °C in methylene chloride.

addition of O_2 to an acetonitrile solution containing equimolar amounts of (F_8TPP)Fe^{II} and [Co^{II}(TMPA)(CH_3CN)]$^{2+}$ at −40 °C, a new spectrum (λ_{max} = 414 (Soret) and 558 nm), was observed. However this product, possibly the putative [Fe^{III}−peroxo−Co^{III}] complex, proved to be very unstable and decomposed rapidly (i.e., seconds) into (F_8TPP)Fe^{III}−OH (λ = 408 (Soret) and 568 nm). Despite efforts made in different solvents and lower temperatures (e.g., propionitrile, acetone, and dichloromethane at −80 °C), a stable μ-peroxo adduct could not be generated or characterized. We also attempted resonance Raman spectroscopic interrogation of the low-temperature oxygenated solutions, but no peroxo species (i.e., with new isotope sensitive O−O stretching vibration in the ∼800 cm^{-1} region) were detected.

Dioxygen Chemistry of [(TPP)Co^{II}]/[Co^{II}(TMPA)-(CH_3CN)]$^{2+}$. The remaining question about the capability of the [Co^{II}(TMPA)(CH_3CN)]$^{2+}$ precursor to form hetero-binuclear metalloporphyrinate with non-porphyrin metal dioxygen adducts was addressed by substituting the heme precursor by the complex (TPP)Co^{II}. It is known that (porphyrinate)−Co^{II} complexes react with O_2 in the presence of a Lewis base as porphyrinate axial ligand (e.g., pyridines and imidazoles) yielding superoxo-Co^{III} complexes, [(porphyrinate)−Co^{III}($O_2^{-\cdot}$)].[40] In the absence of the added base, the [(porphyrinate)−Co^{II}] is inert to O_2.[44]

Remarkably, equimolar amounts of [(TPP)Co^{II}] and [Co^{II}(TMPA)(CH_3CN)]$^{2+}$ react with O_2 in a dichloromethane solution at −80 °C in the absence of a base. The reaction with dioxygen is followed by noticeable changes in the UV−vis spectral features of the original solution; the Soret band is shifted from 413 to 435 nm, and the alpha band at 528 nm changes to 548 nm with a new weak absorption also being observed at 583 nm (Figure 6). Also noteworthy is the fact that by warming up the solution the original spectrum reappears indicating that the reaction is reversible and that the reduced temperature facilitates binding to form what we formulate as the μ-peroxo complex **3** (see Scheme 3).

Scheme 3

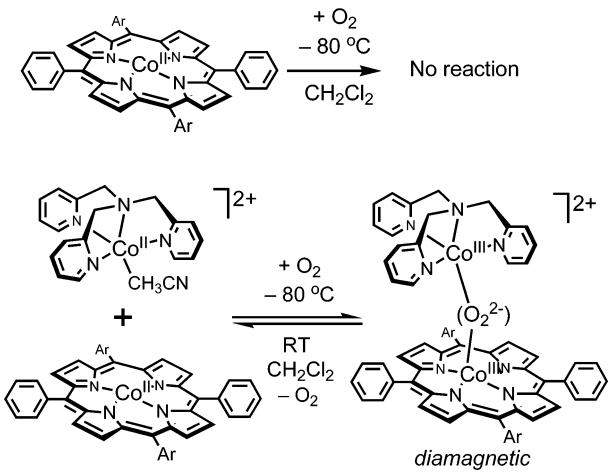

Compelling evidence supporting this formulation and stated stoichiometry of the reversible reaction (Scheme 3) is the observation that we detect close to 1 equiv of O_2 being released from the −80 °C solutions **3** that have been purged of any excess dioxygen and then warmed; see Experimental Section. (Note: repeated attempts to obtain resonance Raman spectroscopic confirmation of the peroxo formulation were not successful.) Each oxygenation cycle is complete (i.e., full formation of the new species, λ_{max} = 435 nm, Figure 6) in less than 5 min for a 3.0 × 10^{-5} M solution. This is very fast by comparison to the time normally required to oxygenate porphyrinate-Co^{II} complexes in the presence of bases.[44]

The same reaction was followed by electron paramagnetic resonance (EPR) spectroscopy. The spectrum (20 K, CH_2Cl_2) of the reduced [(TPP)Co^{II}]/[Co^{II}(TMPA)(MeCN)]$^{2+}$ mixture appears as a composite of the expected spectra for these EPR active high-spin Co^{II} complexes.[25,45,46] However, the product of oxygenation is EPR silent, with a small amount of paramagnetic impurity (at 3350 G) perhaps arising from the presence of some (TPP)Co^{III}($O_2^{-\cdot}$) (see Figure S9, Supporting Information). Thus, observed UV−vis spectral changes combined with evidence from EPR spectroscopy support the formation and formulation of **3** as a low-spin diamagnetic compound[17,47] (also see ^{1}H NMR characterization, below). The presence of a number of other possible species can be ruled out:[47] the peroxo-bridged dimer [(TPP)Co^{III}]$_2$(O_2^{2-}) from [(TPP)Co^{II}]/O_2 is not known. We can rule out the formation of a superoxo species (base)(TPP)-Co^{III}($O_2^{-\cdot}$) because we generated an authentic complex, (1,5-dicyclohexylimidazole)(TPP)Co^{III}($O_2^{-\cdot}$), by mixing the components at the same concentration (1 mM) and solvent; this species is EPR active (see Figure S9) unlike **3**. Another possibility to consider is that only Co^{II}(TMPA) chemistry is involved; although [Co^{II}(TMPA)(CH_3CN)]$^{2+}$ reacts with O_2

(43) Rybak-Akimova, E. V.; Otto, W.; Deardorf, P.; Roesner, R.; Busch, D. H. *Inorg. Chem.* **1997**, *36*, 2746−2753.
(44) Yang, J. P.; Huang, P. C. *Chem. Mater.* **2000**, *12*, 2693−2697.
(45) Assour, J. M. *J. Chem. Phys.* **1965**, *43*, 2477−2489.
(46) Walker, F. A. *J. Am. Chem. Soc.* **1970**, *92*, 4235.
(47) A reviewer has suggested consideration of the formulation of **3** as being a μ-(hydr)oxo-bridged dicobalt(III) complex or a bis-μ-oxo dicobalt(IV) complex. The former can be ruled out since O_2 is evolved upon warming **3**. The latter cannot be completely ruled out, but such a species is unprecedented (however evolution of O_2 from a bis-μ-oxo-dicopper(III) complex is known, see H. Hayashi et al., *J. Am. Chem. Soc.* **2000**, *122*, 2124−2125.).

to form a μ-peroxo complex (unpublished observations), the UV−vis changes observed here (Soret absorption shift, *vide supra*) clearly indicate the presence of a porphyrin moiety which is involved and undergoing reaction/change.

The formation of **3** was also monitored by ^{1}H NMR spectroscopy at −80 °C in dichloromethane-d_2. The spectrum of the starting mixture [(TPP)Co^{II}]/[Co^{II}(TMPA)(CH$_3$CN)]$^{2+}$ shows the paramagnetically shifted signals for both complexes, moved further (up or downfield) from the established room-temperature chemical shifts[48] (See Supporting Information Figure S10). Following the addition of excess O_2, the starting material resonances disappear and new absorptions are observed in the diamagnetic region (Figure S10**)** consistent with the formulation of a low-spin Co^{III} (d^6)−peroxo−Co^{III} (d^6) compound. A binuclear complex derived only from the oxygenation of [Co^{II}(TMPA)(MeCN)]$^{2+}$ can be ruled out as the main product (based on the UV−vis criterion mentioned above) as well as from NMR spectroscopy.[49]

One could speculate on the possibility that a detached (unligated) pyridyl ligand arm from [Co^{II}(TMPA)(MeCN)]$^{2+}$ acts as an axial base for stabilization of a [base−(TPP)Co^{III}-($O_2^{-\cdot}$)] species. However, both the reaction time frame (which is very fast compared to that known for [(base)-(porphyrinate)−Co^{III}−($O_2^{-\cdot}$)] formation),[44] as well as just the fact that [Co^{II}(TMPA)(CH$_3$CN)]$^{2+}$ is involved (i.e., the ^{1}H NMR peaks for Co^{II}(TMPA) disappear), rule out this supposition.

As previously mentioned, [(TPP)Co^{II}] is unreactive toward O_2 without a base, and there is no base present here. Thus, chemical reasoning would suggest that **3** may form via initial reaction of [Co^{II}(TMPA)(CH$_3$CN)]$^{2+}$ with O_2 to give a metastable [(TMPA)Co^{III}($O_2^{-\cdot}$)]$^{2+}$ species that now is reactive toward [(TPP)Co^{II}], leading to **3**.

Conclusions and Summary

With our ongoing studies and previous characterization of a series of [(porphyrinate)Fe^{III}−X−Cu^{II}(ligand)]$^{n+}$ [X = O^{2-} (oxo), $(OH)^-$ (hydroxo), O_2^{2-} (peroxo)] complexes, our goal here was to investigate the effect of cobalt ion substitution for copper or copper and iron. As studied especially by Collman and Boitrel,[15−17] interesting variations might be expected, in particular, with respect to the potential stabilization of superoxo and/or peroxo intermediates by virtue of the possible generation of Co^{III} species with resulting 3d^6 electronic configuration. Because our program has enjoyed particular success in the derivation of these bridged complexes via dioxygen reactivity with reduced Fe^{II} or Cu^{I} components, we wished to explore such chemistry when Co^{II} was involved. Our efforts were partially successful, and the investigations have given rise to new μ-oxo, μ-hydroxo, and μ-peroxo complex chemistry. The main findings of the present report are as follows:

(1) Our previous kind of Fe^{II}/Cu^{I}/O_2 chemistry was carried out but now with a cobalt analogue; however, [(F$_8$TPP)Fe^{III}−peroxo−Co^{III}(TMPA)]$^{2+}$ either does not form or is very unstable.

(2) A μ-oxo complex (**1**) was, however, generated by acid−base assembly and its X-ray structure determined. Structural comparisons with analogue [Fe^{III}−O−Cu^{II}] and other μ-oxo metal complexes were made.

(3) The magnetic properties of μ-oxo complex **1** were deduced and comparisons with [Fe^{III}−O−Fe^{III}] and [Fe^{III}−O−Cu^{II}] analogues were made. The latter showed to be more strongly magnetically coupled.

(4) A μ-hydroxo complex (**2**) is formed by addition of 1 equiv acid to the μ-oxo complex **1**. Production of **2** was also proved to be completely reversible by addition of a base (triethylamine).

(5) Formation of an asymmetric μ-peroxo complex (**3**) was accomplished by dioxygen chemistry of [(TPP)Co^{II}]/[Co^{II}-(TMPA)(MeCN)]$^{2+}$ at low temperature. It was also found that the oxygenation/deoxygenation equilibrium is reversible and that the original reduced complexes and dioxygen can be recovered by increasing the temperature.

Experimental Section

Materials and Methods. Reagents including the *meso*-tetraphenylporphyrin Co^{II} complex were used as received from commercial sources or otherwise noted. Acetone was predried and distilled over Dreirite. Acetonitrile was predried and distilled over fresh CaH_2. Dichloromethane was purified through an alumina column. The solvents were deoxygenated by direct argon bubbling (30 min) or by five freeze/pump/thaw cycles. The air- and moisture-sensitive samples were handled and stored using standard Schlenk glassware and drybox facilities. Elemental analyses were performed by QTI Inc. (Whitehouse, NJ). Infrared spectra were measured from 4000 to 400 cm^{-1} as KBr pellets on a Mattson Galaxy 4030 Fourier transform (FT) IR spectrometer. Blank spectra were recorded to ensure the anhydrous character of the KBr matrix. ^{1}H NMR spectra were carried out using a Varian unit 400 MHz FT−NMR spectrometer. Mass spectrometry (ESI in the positive ion mode) was measured on a Thermo-Finnigan LCQ Deca. Low- and room-temperature UV−vis spectra in the range of 200−1200 nm were recorded on a diode array HP-8453 UV−vis spectrophotometer interfaced with a Neslab refrigerated circulating bath. The temperature-dependent susceptibility measurements of the Co-precursors were performed in the range of 2−295 K at 1 T on a *Quantum Design* MPMS SQUID-magnetometer. The Heisenberg−Dirac-van Vleck (HDvV) model was used to analyze the data, and the fitting of the temperature-dependent magnetization was carried out using a least-squares fitting computer program[50] as reference with a full matrix diagonalization approach. The software uses the spin Hamiltonian operator $\mathbf{H}_{total} = \mathbf{H}_Z + \mathbf{H}_{ZFS} + \mathbf{H}_{HDvV}$, where the exchange coupling is described by $\mathbf{H}_{HDvV} = -2JS_1 \times S_2$, the Zeeman interactions are given by $\mathbf{H}_Z = \mu_B B g_i S_i$ and the axial single-ion zero-field interaction is described by $\mathbf{H}_{ZFS} = DS_Z^2$. The ligand TMPA and the synthons (F$_8$TPP)Fe^{II}·H$_2$O and (F$_8$TPP)Fe^{III}OH were synthesized following minor modifications of previously published procedures.[5,9,51]

(48) La Mar, G. N.; Walker, F. A. *J. Am. Chem. Soc.* **1973**, *95*, 1790−1796.

(49) Unpublished observations show that [Co^{II}(TMPA)(MeCN)]$^{2+}$ reacts with O_2 to give a diamagnetic binuclear peroxo complex with a distinctive broad ^{1}H−NMR resonance in the 3−4 ppm region (Figure S11, Supporting Information). This is observed to form in about a 15−20% yield under the reaction conditions described for the formation of **3**.

(50) Krebs, C. Thesis, Ruhr-Universität, Bochum, Germany, 1997.

(51) Tyeklár, Z.; Jacobson, R. R.; Wei, N.; Murthy, N. N.; Zubieta, J.; Karlin, K. D. *J. Am. Chem. Soc.* **1993**, *115*, 2677−2689.

[Co^{II}(TMPA)(CH$_3$CN)](ClO$_4$)$_2$. TMPA (0.58 g: 2.00 mmol) was added to a dry Schlenk flask containing deaerated acetonitrile (40 mL). After the contents of the flask were homogenized, [Co^{II}(H$_2$O)$_6$](ClO$_4$)$_2$ (0.73 g: 2.00 mmol) was introduced and a purple solution was generated. Air-free diethyl ether (100 mL) was slowly added after 2 h to help precipitation. The microcrystalline product was filtered and then dried for 48 h. Yield was 0.92 g (80%). IR (KBr, cm^{-1}); 3066 (C−H stretch), 2344−2371 (w, C≡N stretch), 1611 (s, C═C$_{Py}$ stretch), 1439 (CH$_{2Py}$ scissor vib), 1091 (s, br ClO$_4^-$), 781−767 (C−H$_{Py}$ out-of-plane), and 624 (C═C$_{Py}$ rock). ESIpos: [M − MeCN − ClO$_4$]$^+$ *m*/*z* = 448; [M − MeCN − 2ClO$_4$]$^+$ *m*/*z* = 175. Elemental analysis (C$_{20}$H$_{21}$N$_5$O$_8$Cl$_2$Co$_1$, 589.25 g/mol) calc/found C: 40.77/40.8; H: 3.59/3.6; N: 11.89/11.7. UV−vis (MeCN) 472 nm (ϵ = 82 M^{-1}·cm^{-1}), 552 nm (ϵ = 52 M^{-1}·cm^{-1}), and 945 nm ($\epsilon \leq 5$ M^{-1}·cm^{-1}). ^{1}H NMR [400 MHz, CD$_2$Cl$_2$, 300 K] δ(ppm) = 109.1 [−CH$_2$−], 60.7 [5-H], 41.6 [3-H], and −4.6 [4-H] (Note these are new, corrected values, see above text).

Preparation of 1. In an argon atmosphere the synthons (F$_8$TPP)Fe^{III}OH (0.166 g : 0.20 mmol) and [Co^{II}(TMPA)(CH$_3$CN)](ClO$_4$)$_2$ (0.120 g: 0.20 mmol) were combined in a 50 mL flame-dried Schlenk flask and stirred for 1 h to foster intimate contact. Previously deaerated dichloromethane (30 mL) was added, and the solution was stirred for 1 h. When Et$_3$N (35 μL: 0.25 mmol) was added, the original brownish solution immediately became reddish. After 15 min the volume was reduced to one third and anhydrous, air-free toluene (∼20 mL) was added. The microcrystalline product was filtered and then vacuum-dried for 48 h. Yield was 0.25 g (∼80%). IR (KBr, cm^{-1}); 1622−1608 (s, C═C$_{pyridine}$ stretch), 1463 (pyrrole ring stretch), 1092 (br ClO$_4^-$), 999 (C−H$_{pyridine}$ out-of-plane), and 624 (C═C$_{pyridine}$ rock). ESIpos: [M − ClO$_4$]$^+$ multiplet *m*/*z* = 1176.1 (13% relative abundance), 1177.1 (100%), 1178.1 (73%), and 1179.1 (22%); [M − (Co^{II}TMPA) − ClO$_4$ + CH$_3$CN]$^+$ *m*/*z* = 852.5; [M − (Co^{II}TMPA) − ClO$_4$]$^+$ *m*/*z* = 812.5. MALDI-TOF; [M − ClO$_4$]$^+$ *m*/*z* = 1178. Elemental analysis for (**1**)·2CH$_2$Cl$_2$·C$_7$H$_8$ (C$_{71}$H$_{50}$N$_8$Cl$_5$F$_8$O$_5$Fe$_1$Co$_1$, 1539.19 g/mol) calc/found: C = 58.08/58.18; H = 3.43/3.66; N = 7.63/7.48. ^{1}H NMR [400 MHz, CD$_2$Cl$_2$, 300 K] δ(ppm) = 40.6 [pyrrole], 8.8 [*m*-phenyl], 8.7 [*m*-phenyl], 8.0 [*p*-phenyl], 4.4 [4-H$_{py}$], 2.6 [3-H$_{py}$], 1.0 [5-H$_{py}$], −1.1 [6-H$_{py}$], and −2.7 [TMPA−CH$_2$−].

^{1}H NMR Titration. Protonation of 1. In the glovebox, a CD$_2$Cl$_2$ solution of **1** (12 mg, 0.0078 mmol, in 0.7 mL solvent) was prepared and transferred to a screw-cap NMR tube, and the ^{1}H NMR spectrum was recorded. Previously distilled triflic acid (HSO$_3$CF$_3$) was used to prepare a stock solution (21 mg in 2 mL of CD$_2$Cl$_2$). Then, a 50 μL aliquot of acid (0.45 equiv) was introduced to the solution of **1** (using a 250 μL Hamilton syringe), the tube was shaken and the ^{1}H NMR spectrum was recorded. This process of adding aliquots of acid and recording spectra was performed twice more (for 0.9 and 2.6 equiv acid).

NMR Spectroscopy. Room temperature and variable-temperature ^{1}H NMR spectra were recorded on a Varian Unity 400 NMR instrument. All spectra were recorded in 5 mm o.d. NMR tubes. The chemical shifts were reported as δ (ppm) values calibrated to natural abundance proton solvent peak. Typically, (i) 12 mg of **1** or (ii) 8 mg of Co^{II}(TPP)/6 mg of [Co^{II}(TMPA)(CH$_3$CN)](ClO$_4$)$_2$ (equimolar amounts) in ∼ 0.7 mL of CD$_2$Cl$_2$ were used for each experiment.

The ambient temperature solution magnetic moment of **1** was measured by the Evans method[52,53] on a Varian NMR instrument at 400 MHz. Inside a glovebox, a dichloromethane-d_2 solution of **1** with known concentration (4.6 mM) was prepared and placed in a NMR tube. A ^{1}H NMR spectrum was first recorded and then a coaxial reference capillary filled with pure dichloromethane-d_2 was inserted inside the sample tube. A second ^{1}H NMR spectrum was thus obtained (now with a capillary containing pure solvent) and in this manner was assigned unequivocally the solvent peak corresponding to the pure deuterated solvent. Both solvent peaks were assigned, one corresponding to the paramagnetically shifted deuterated solvent and the second corresponding to the pure solvent from the reference capillary. The magnetic moment was calculated from the equation $\mu_B = 2.84\sqrt{\chi_M T/n}$, where T is the temperature (297 K) of the measurement, n is the nuclearity of the complex (n = 1 for **1**), and $\chi_M = -3/4\pi(\Delta\nu/\nu)1000/c + \chi_M^{sol} - \chi_D$ (where χ_M^{sol} is the solvent susceptibility, χ_D is the total diamagnetic correction calculated from Pascal's constants,[54,55] $\Delta\nu$ is the paramagnetic shift of the solvent in Hz, ν is the frequency of the NMR instrument in Hz, and c is the concentration of the metal complex). In the same way the magnetic moment of **2** (prepared by addition of 1 equiv triflic acid to a solution of **1**) and the mixture of (F$_8$TPP)Fe^{III}−(OTf) and [Co^{II}(TMPA)(H$_2$O)]$^{2+}$ (prepared by addition of 2.6 equiv triflic acid to a solution of **1**) were determined.

UV−vis Absorption Spectroscopy. Dioxygen Chemistry of Co^{II}(TPP)/[Co^{II}(TMPA)−(CH$_3$CN)]$^{2+}$. In a typical experiment, equimolar amounts of Co^{II}(TPP) and [Co^{II}(TMPA)(CH$_3$CN)](ClO$_4$)$_2$ were dissolved in CH$_2$Cl$_2$ (3×10^{-5} M) in an inert atmosphere glovebox. The solution was placed in a special UV−vis cuvette,[56] sealed, brought out of the glovebox, and cooled to −80 °C. The solution was oxygenated via bubbling with excess dry O$_2$. The UV−vis spectra before and after oxygenation were recorded.

EPR Spectroscopy. Equimolar amounts of Co^{II}(TPP) and [Co^{II}(TMPA)(CH$_3$CN)](ClO$_4$)$_2$ were dissolved in CH$_2$Cl$_2$ (1 mM) in a glovebox, and the solution was transferred to an EPR tube that was capped with a rubber septum. The EPR tube was immersed in a −80 °C bath (acetone/dry ice) when dry O$_2$ was added via syringe to generate **3**. The solution was frozen in liquid N$_2$, and the X-band EPR spectrum of **3** was recorded on a Bruker EMX spectrometer, with temperature maintained at 20 K using an Oxford Instruments EPR 900 cryostat.

Magnetic Susceptibility Measurements. Temperature-dependent magnetic susceptibility measurements were performed on a Quantum Design SQUID-magnetometer MPMS in the temperature range of 2−298 K in applied magnetic fields of 1 T. The response function was measured four times for each given temperature. The experimental data were corrected for the diamagnetic contribution using Pascal's constants.

Dioxygen Evolution upon Warming a Solution of 3. An alkaline pyrogallol solution was used to detect dioxygen evolution upon warming a solution of **3**, following a previously published protocol.[57,58] In the glovebox, 32.3 mg of [Co^{II}(TPP)] and 28.4 mg

(52) Evans, D. F. *J. Chem. Soc.* **1959**, 2003.

(53) Ghiladi, R. A.; Kretzer, R. M.; Guzei, I.; Rheingold, A. L.; Neuhold, Y.-M.; Hatwell, K. R.; Zuberbühler, A. D.; Karlin, K. D. *Inorg. Chem.* **2001**, *40*, 5754−5767.

(54) O'Connor, C. J. In *Progress in Inorganic Chemistry*, Vol 29; John Wiley & Sons Inc: New York, 1982, pp 203.

(55) *CRC Handbook of Chemistry and Physics*, 80th ed.; CRC Press: London, 1999.

(56) Karlin, K. D.; Haka, M. S.; Cruse, R. W.; Meyer, G. J.; Farooq, A.; Gultneh, Y.; Hayes, J. C.; Zubieta, J. *J. Am. Chem. Soc.* **1988**, *110*, 1196−1207.

(57) Kim, E.; Helton, M. E.; Lu, S.; Moënne-Loccoz, P.; Incarvito, C. D.; Rheingold, A. L.; Kaderli, S.; Zuberbühler, A. D.; Karlin, K. D. *Inorg. Chem.* **2005**, *44*, 7014−7029.

(58) Ghiladi, R. A.; Huang, H. W.; Moënne-Loccoz, P.; Stasser, J.; Blackburn, N. J.; Woods, A. S.; Cotter, R. J.; Incarvito, C. D.; Rheingold, A. L.; Karlin, K. D. *J. Biol. Inorg. Chem.* **2005**, *10*, 63−77.

of $[Co^{II}(TMPA)(CH_3CN)](ClO_4)_2$ were dissolved in 20 mL of deoxygenated CH_2Cl_2 and transferred to a 50 mL Schlenk flask equipped with a stir-bar and capped with a rubber septum. Outside the glovebox, the solution was cooled to −78 °C in a dry ice/acetone cold bath, and then the peroxo complex **3** was generated by direct bubbling of dry O_2 through the solution via syringe. The solution was allowed to stand in the cold bath for several minutes to ensure complete formation of **3**, and after that the solution was degassed via three freeze−pump−thaw cycles to remove any free O_2. In the meantime, an alkaline pyrogallol solution [4.0 g of pyrogallol (1,2,3-trihydroxybenzene) in 25 mL of deoxygenated 50% $KOH_{(aq)}$ solution] was freshly prepared in a modified 100 mL Schlenk flask possessing a 2 mm path length cuvette. The alkaline pyrogallol solution started out with a faint beige color, and its UV−visible spectrum was recorded. The solution of **3** was then allowed to warm to room temperature. Next, using a syringe needle, argon was slowly passing through the headspace of the Schlenk flask containing the solution of **3** (now decomposed), thus moving the liberated O_2 through a cannula to the other Schlenk flask containing the alkaline pyrogallol solution. The liberated O_2 was bubbled directly into the pyrogallol solution whose color began to darken after 2−3 min. After 20−30 min of purging the flask with argon, the pyrogallol ceased becoming darker, and its UV−vis spectrum was re-recorded. The published calibration curve,[58] absorbance (400 nm) = (0.0716 × mL O_2) + 0.025, was used to determine the amount of dioxygen evolved upon thermal decomposition of **3**. Two reaction runs produced 75 and 82% yields of O_2 based on the stated stoichiometry, Scheme 3.

Acknowledgment. This work was supported by grant from National Institutes of Health (GM 34909, (to K.D.K.) and by a grant from the Deutsche Forschungsgemeinschaft, DFG (to E.R. and U.S.)

Supporting Information Available: Crystal data for **1** (Table S1); ESI mass spectrum and calculated spectrum of **1** (Figures S1 and S2); ^{1}H NMR spectrum of $[Co^{II}(TMPA)(MeCN)]^{2+}$ (Figure S3); variable temperature ^{1}H NMR spectra and Curie plot of **1** (Figures S4 and S5); protonation/deprotonation cycles of **1** followed by UV−vis spectroscopy (Figure S6); protonation of **1** followed by ^{1}H NMR spectroscopy (Figure S7); reversible acid−base conversion of **1** by adding 2 equiv of HOTf and 2 equiv of Et_3N and monitored by UV−vis spectroscopy (Figure S8); EPR spectra of **3** and an authentic [(1,5-dicyclohexylimidazole)(TPP)$Co^{III}-O_2^{-\cdot}$] (Figure S9); reactions $[Co^{II}(TPP)]/[Co^{II}(TMPA)(MeCN)]^{2+}/O_2$ and $[Co^{II}(TMPA)(MeCN)]^{2+}/O_2$ followed by ^{1}H NMR at −80 °C (Figures S10 and S11, respectively). This material is available free of charge via the Internet at http://pubs.acs.org.

IC061686K